Power System Technology
ISSN:1000-3673

Received: 16-01-2024 Revised: 12-02-2024 Accepted: 27-03-2024

Crush Analysis of External Inversion of Tubes with Variable Thickness Distribution

Vahid Yousefi Ramandi[1], Mahmoud Mosavi Mashhadi [2*], keivan Hosseini Safari[3] and Mohammad Mahdi Kheirikhah[4]

[1,2,4] Department of Mechanical Engineering, Qazvin Branch, Islamic Azad University, Qazvin, Iran

[3] Department of Mechanical Engineering, Central Tehran Branch, Islamic Azad University, Tehran, Iran.

*Corresponding author: Mahmoud Mosavi Mashhadi Email: mmosavi@ut.ac.ir

Abstract:

Axial crush tests on Uniform Thickness (UT) and Functionally Graded Thickness (FGT) tubes have been performed for external inversion process, and crashworthiness performance, and benefits of FGT tubes compared with their UT equivalents. Furthermore, in order to find detail verification about crush process of FGT tubes, Finite element (FE) models developed using explicit FE code under axial loading. Then, these FE models validated by experimental tests to ensure that they can accurately predict the responses of FGT inversion tubes. Our study shows that tube thickness distribution, die radius, and coefficient of friction between die and tube have great influence on the responses of FGT tubes inversion. The results give new design ideas to improve crashworthiness performance of inversion tubes.

Keywords*: Inversion tube, Functionally Graded Thickness, Finite element model, Axial crushing*

1. Introduction

Thin-walled metallic tubes are efficient collapsible energy absorbers and they widely used as energy absorbers in crashworthiness applications such as automotive and aerospace industries to protect passengers and machinery from endanger. Alternatively, thin walled crush absorbers are light weight structures that are important factor to reduce the fuel consumption of vehicles and improve air quality. Numerous efforts have been made in the past decades to improve the crashworthiness performance of the crush absorber tubes, such as foam filled tubes [1-5], introducing different patterns [6], grooves [7-8], multi-cells [9-10] and functionally graded structures [11-13].

An inversion tube is able to absorb high energy under certain conditions. Inversion is a mode of plastic deformation which develops, when a thin walled tube is compressed between a flat

Power System Technology
ISSN:1000-3673
Received: 16-01-2024 Revised: 12-02-2024 Accepted: 27-03-2024

plate at one end and fileted die at other [14-15]. Recently, many applications of inversion tubes have been made. Such as, force actuating collapsible steering wheels, cushioning air drop cargo, helicopter seats and soft landing of spacecraft [16]. Experimental studies and theoretical analysis on tube inversion have been conducted by many researchers in the recent decades. Al-Hassani et al [17], Reid [18] and Reddy [19] made experimental investigations and theoretical analysis for the deformation behavior and forming load of external inversion. Miscow et. al. [20] studied the theoretical and experimental studies of the static and dynamic inversion process in circular tubes. This theoretical analysis is valuable as the first formula that predicts the axial force versus the axial displacement during the inversion process. But, theoretical curve that sketched based on the Miscow's theory shows an intensive increment at the onset of loading with a large difference, comparing the experimental curve. The effects of strain rate and inertia during dynamic free inversion process were further investigated by Colokoglu and Reddy [21]. However, the prediction process is very complicated and generally, theory and experiments have not acceptable agreements with each other. Accordingly, the predicted quasi-static inversion load is significantly lower than experimental value while the predicted dynamic mean load is overestimated. Recently, Sekhon et al. [22] and Rosa et al. [23] used the general finite element software to analyze external inversion over filleted die.

Reviewing the literature, presents that an effective way to increase the energy absorption of a structure is to harden the material and simultaneously increase the thickness during the forming process [14-19]. Up to now, there is no study on inversion process in thin-walled tubes structures with axial distributed variable thickness. In this paper, the crush performance of the various FGT inversion tubes is investigated under axial loading through the several quasi-static tests. Then, numerical simulations of the crush tests were performed to obtain detail information about the crush performance of the FGT tubes by LS-DYNA. To fully understand and quantify the energy absorption behavior of FGT tubes, a parametric study has been undertaken with reference to the geometry parameters through validated FE model on FGT inversion tube with die and uniform circular without die. This study gives new design information for tubes inversion and shows that under specific conditions, energy absorption performance of FGT inversion tubes are better than uniform tubes.

2. Methodology

2.1 Problem description and specimen preparation

As illustrated in the schematics in Figure 1, two different structural configurations, namely UT and FGT tubes are studied in this paper. Where, the mathematical expression for grading thickness distribution of FGT tube is given by

$$T(y) = t_1 + (t_2 - t_1)\left[\frac{x}{L_\alpha}\right]^m \quad (1)$$

Power System Technology
ISSN:1000-3673
Received: 16-01-2024 Revised: 12-02-2024 Accepted: 27-03-2024

Here, all of the tubes have the same baseline dimensions with length $L = 75\,mm$ and outer diameter $D = 50\,mm$. It is first assumed that the FGT tubes have a linearly graded thickness from $t_1 = 1$ mm to $t_2 = 2$ mm, and the UT tubes have an equivalent thickness of $t = 2$ mm. Also, the terms α and L_α in Figure 1 are angle and length of tube section with distributed thickness.

Where x is the distance from bottom to the height L_α, and m is the order of thickness distribution, with m=1 for linear variation of tube thickness.

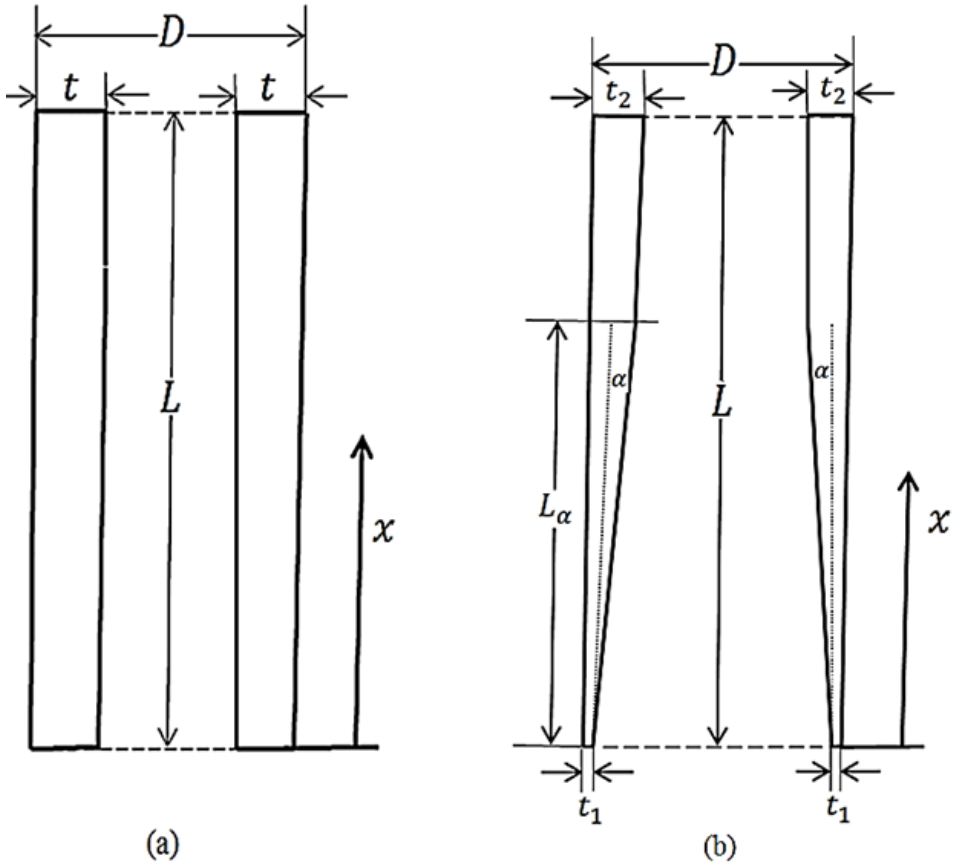

Figure 1. Schematic view of the test specimens,
(a) uniform tube UT,(b) functionally graded thickness FGT tube

Three different tube profiles with angles $\alpha = 1°, 2°$ and $3°$ are investigated here and three specimens are prepared for each case (Figure 2). As shown in Figure 1, L_α in specimens for three different angles can be calculated as follow:

$$L_\alpha = \frac{t_2 - t_1}{\tan \alpha} \tag{2}$$

So, L_α for three different angles are calculated as $L_{\alpha=1°} = 57.2\,mm$, $L_{\alpha=2°} = 28.63\,mm$, $L_{\alpha=3°} = 19.08\,mm$.

Power System Technology
ISSN:1000-3673
Received: 16-01-2024 Revised: 12-02-2024 Accepted: 27-03-2024

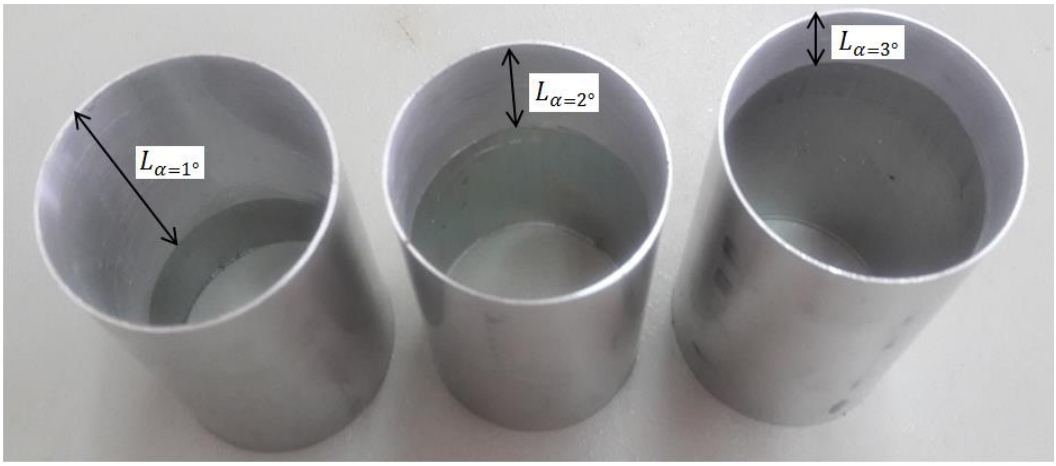

Figure 2. Specimens of f FGT tubes for three different angles $\alpha = 1°, 2°$ and $3°$

2.2 Material properties

The Circular aluminum alloy AA6061 tubes utilized for experimental tests. To obtain tubes exact stress–strain curve and mechanical properties, three similar specimens prepared from tubes in longitudinal direction based on ASTM standard tensile test (Figure 3) [24]. The strain rate was $2.77 \times 10^{-3}\ s^{-1}$. The mechanical properties of aluminum alloy AA6061 are tabulated in Table 1.

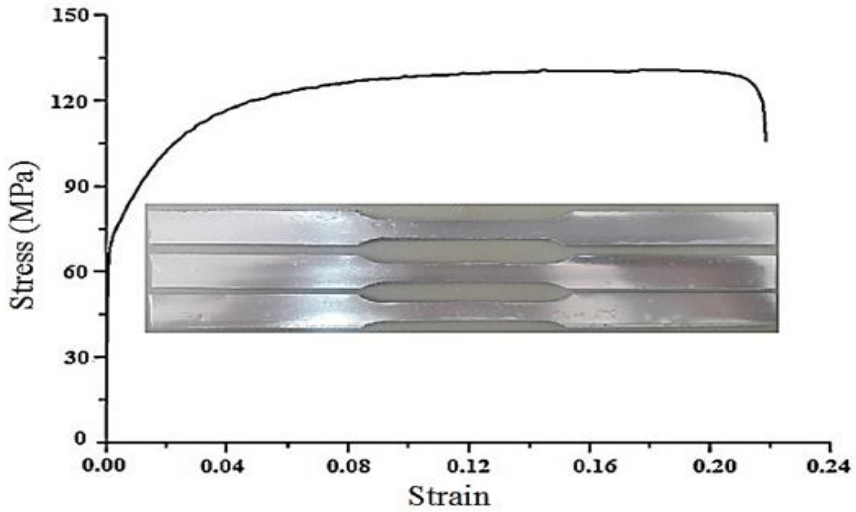

Figure 3. Engineering stress–strain curve of aluminum alloy AA6061

Power System Technology
ISSN:1000-3673
Received: 16-01-2024 Revised: 12-02-2024 Accepted: 27-03-2024

Table 1. The tensile mechanical properties of aluminum alloy AA6061

Mechanical Properties	Young's Modulus E	Yield Strength $\sigma_{0.2}$	Ultimate tensile Strength	Poison Ratio ϑ	Failure Strain %
Value	68.4 GPa	75.8 MPa	130 MPa	0.3	22

2.3 Finite Element FE model

Developing an accurate FE analysis, proper selection of the impact modeling technique will have great contribution on crashworthiness analysis. Here, the crush behavior of UT and FGT tubes is studied to predict their main crashworthiness features as function of the tube material and geometrical parameters. The FE analysis is employed to find these behaviors for various cases which are difficult and expensive to perform by experimental tests. The finite element models of the tubes were developed with the use of commercial explicit finite element code LS-DYNA. Aluminum alloy is modeled by applying the piecewise linear elastic–plastic material model with the constitutive equation of strain hardening as [18]:

$$\dot{\varepsilon} = D\left(\frac{\sigma_0'}{\sigma_0} - 1\right)^q \tag{3}$$

In which σ_0' is the dynamic flow stress at a uniaxial plastic strain rate, σ_0 is the associated static flow stress, and the constants D and q are material parameters. These parameters are selected for aluminum 6061 as $D = 1{,}288{,}000$ and $q = 4$ [18]. The yielding function is defined by the von-Mises yielding criterion as:

$$\varphi = \frac{1}{2}S_{ij}S_{ij} - \frac{\sigma_y}{3} \tag{4}$$

Where S_{ij} and σ_y are the deviatoric stress and the current radius of the yield surface. As illustrated in Figures 4 and 5, the full section FGT and UT tubes are modeled by the quadrilateral Belytschko-Tsay shell element with four nodes and three integration points considered throughout the thickness. Top and bottom plates modeled as rigid bodies. It is assumed that bottom die is fixed and the top plate only moves in longitudinal direction and has one degree of freedom. The optimum mesh size for each simulation is obtained after performing the mesh sensitivity analysis. It indicates that an element size of 3 mm (3200 elements in FE model) is adequate to produce suitable results. In the other words, the mesh size is suitable when the obtained results are logical for crush simulation and do not change drastically.

The automatic single surface contact algorithm is used to account the contact force between the crush zone surfaces or metal folds. The node to surface algorithm models the contact between the rigid plate (die) and the crushed components. The friction coefficients at the different interfaces have been taken $\mu = 0.2$. In all simulations the die radius is $r = 3\ mm$. To obtain the appropriate value of friction factor μ_d between die and tube interface, various values

Power System Technology
ISSN:1000-3673
Received: 16-01-2024 Revised: 12-02-2024 Accepted: 27-03-2024

for μ_d was tested. It is seen that when, $\mu_d = 0.02$ was utilized, the load-displacement curves and deformed shapes of tubes are similar to the experimental tests. Therefore, the value of friction coefficient $\mu_d = 0.02$ assumed for subsequent study.

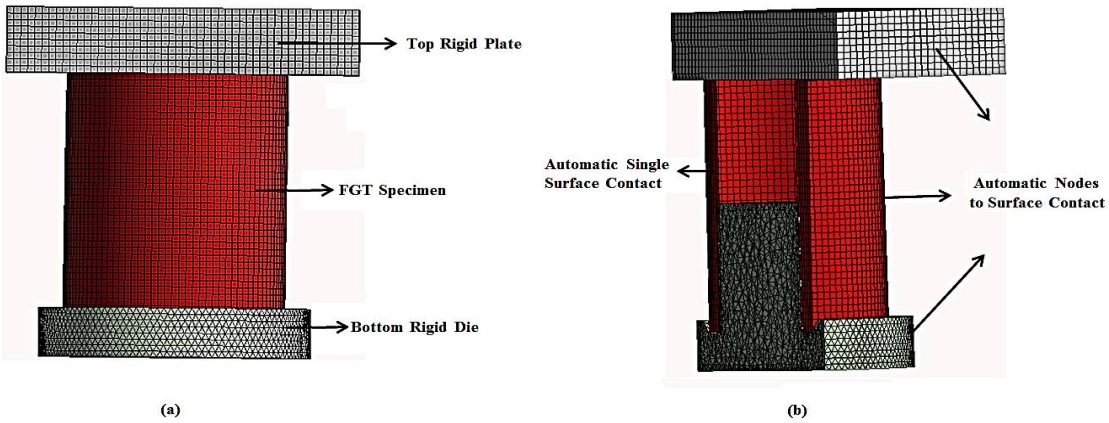

Figure 4. The details of representative finite element model for FGT inversion tube with die and uniform circular without die; (a) overall view, (b) cross-sectional view

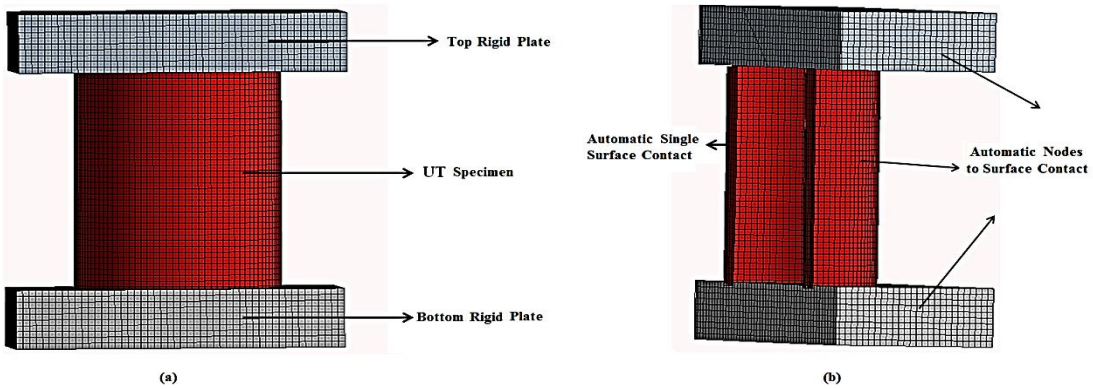

Figure 5. The details of representative finite element model for UT tube without die; (a) overall view , (b) cross-sectional view

2.4 Experimental test

This section describe experimental test used to validate the FE models under axial loading. Quasi-static compression tests of specimens have been done using the 250 kN standard tensile-compression test machine (Figure 7). The top plate feed rate is considered as 3 mm/min with maximum 40mm progress. Friction plays a significant role to ensure the process of tube inversion to deform. Grease based on lithium soap was used during experiment to reduce the friction factor and preventing folding mode of tube crush. The die surface and inner area of the tubes has been lubricated with grease before conducting the experiments. As depicted in Figure 8, in order to compare FGT and UT tubes crush responses with each other, only FGT

Power System Technology
ISSN:1000-3673
Received: 16-01-2024 Revised: 12-02-2024 Accepted: 27-03-2024

tubes with linear variation of thicknesses and constant angles $\alpha = 1°, 2°$ and $3°$ are tested (Figure 7). Then, the validated FE model was used to consider metallic tubes with various geometries by parametric study.

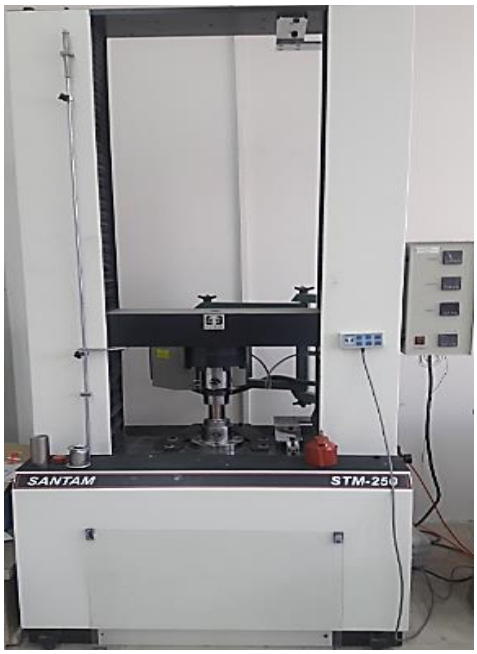

Figure 6. Standard tensile-compression test for quasi-static loading

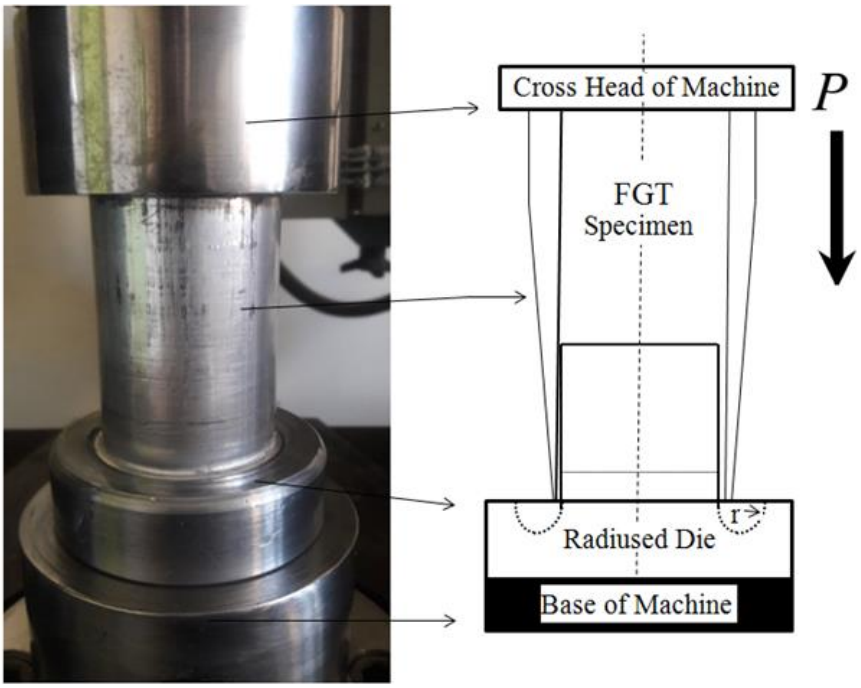

Figure 7. Experimental set up and the die used for studying the external inversion process of FGT tubes

Power System Technology
ISSN:1000-3673
Received: 16-01-2024 Revised: 12-02-2024 Accepted: 27-03-2024

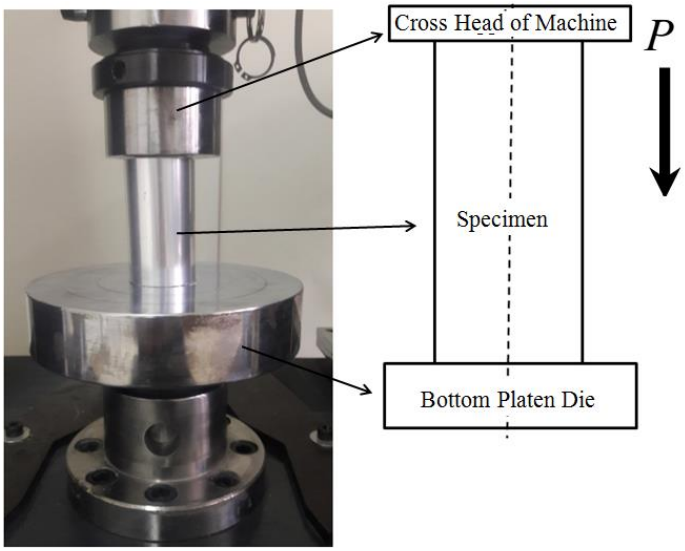

Figure 8. Experimental set up used for studying uniform thickness tube without die

3. Results and discussions

3.1 Experimental results and FE model validation

The FE result of the UT tube without die and FGT tubular specimens under axial loading condition compared and validated by experimental results. The final crushed shape of UT and FGT tubes are shown in Figure 9-a to Figure 9-d. In the Figure 9-a, both experimentally and numerically, it is seen that UT tube without die the folding begins, from the upper section, and continues with stacking more folding during the crushing. Also, as depicted in Figure 9-b to Figure 9-d different deformation modes are observed in FGT tubes with linearly variable thicknesses. In, all three FGT specimens with angles $\alpha = 1°, 2°$ and 3° tubes thickness starts from t_1=1 mm at bottom side to maximum t_2=2 mm at height L_α (Figure 1). Because of relatively smaller cross section of the FGT tubes in the bottom side, compression load results higher stress rates at this side and deformation of all FGT specimens start from the bottom by inversion of tubes. But, approximately, after reaching to the height of L_α, inversion process changes to folding of tubes. Therefore, complete inversion of tube only occurs in the FGT tube with $\alpha = 1°$ with $L_{\alpha=1°} = 57.2\,mm$ that is greater than 40 mm maximum compression progress. The comparison between load vs. displacement between experimental and FE simulation is shown in Figure 10. The predicted load–displacement curve shows acceptable agreement with experimental curves.

For better comparing the results of finite element energy absorption characteristic of UT tube and FGT tube with the experimental results, various results are presented in Table 2. Specified Energy Absorption (SEA) is an important design criterion, and is given by:

Power System Technology
ISSN:1000-3673
Received: 16-01-2024 Revised: 12-02-2024 Accepted: 27-03-2024

$$SEA=\frac{\int_0^d Fdx}{m_c}=\frac{E}{m_c} \quad (5)$$

Where, m_c is the total mass of the component and E is energy absorbed. In table 2, P_{max} (peak load), P_m (mean load), E and SEA in various tube geometries are calculated by FE simulation and compared with the experimental tests. The FE simulation results indicate acceptable agreement with experiments.

Figure 9. Experimental and FE simulation deformation pictures, (a) UT tube, (b) FGT tube with lathe angles $\alpha = 1°$, (c) FGT tube with lathe angles $\alpha = 2°$, (d) FGT tube with lathe angles $\alpha = 3°$

Power System Technology
ISSN:1000-3673

Received: 16-01-2024 Revised: 12-02-2024 Accepted: 27-03-2024

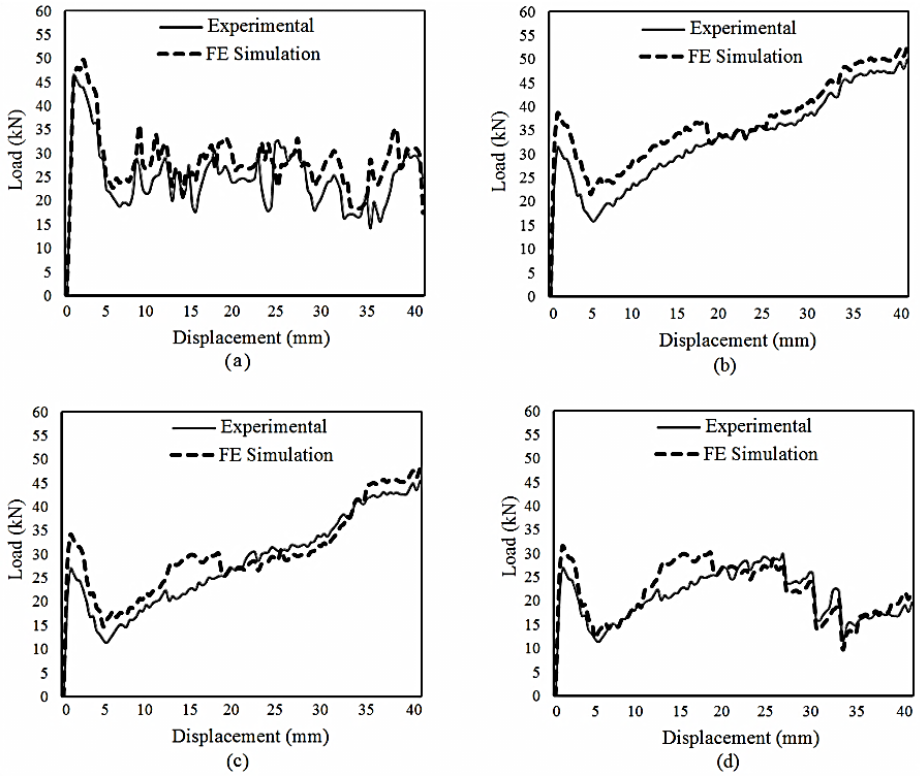

Figure 10. Experimental and simulation load-displacement curves, (a) UT tube, (b) FGT tube with lathe angles $\alpha = 1°$, (c) FGT tube with lathe angles $\alpha = 2°$, (d) FGT tube with lathe angles $\alpha = 3°$

Table 2. Experimental and FE simulation results for various types of tubes
Exp: Experimental results, FE: Finite Element results, Diff: Difference

Tube Case	$P_{max}(kN)$			$P_m(kN)$			E (kJ)			SEA(kJ/kg)		
	Exp.	FE	Diff. (%)	Exp.	FE	Diff. (%)	Exp.	FE	Diff. (%)	Exp.	FE	Diff. (%)
UT	47.9	52.4	8.5	28.1	33.4	15.8	1.6	1.9	15.7	32.4	38.5	15.8
FGT ($\alpha = 1°$)	47.4	53.9	12.6	39.3	42.9	7.2	2.1	2.5	16	43.9	48.6	9.6
FGT ($\alpha = 2°$)	43.6	49.2	11.3	37.8	45.2	16.3	1.9	2.3	17.3	38.2	42.3	10.7
FGT ($\alpha = 3°$)	28.4	33.6	15.4	31.1	35.6	7.5	1.8	2.1	14.2	37.6	41.9	10.2

Power System Technology
ISSN:1000-3673
Received: 16-01-2024 Revised: 12-02-2024 Accepted: 27-03-2024

From experimental results represented in Figure 10 and table 2, it is seen that load-displacement curve in the complete inversion process for FGT tube with $\alpha = 1°$ is smoother than the UT tube with folding crush behavior, and meanwhile SEA=43.9 and mean force P_m=39.3 kN of FGT tube with $\alpha = 1°$ is meaningfully more than SEA=32.4 P_m=28.1 kN for UT tube with the same overall dimensions. Beside on, initial peak force in the FGT tubes is lower than UT tube. Therefore, using suitable FGT tubes guarantees full inversion process with better crush characteristics and behavior.

3.2 Parametric study

Using the finite element modeling in Section 2.3 and based on the performance indices given in Section 3.1, the energy absorption characteristics of the proposed FGT inversion tubes is parametrically compared with the UT tubes. The process of external inversion of FGT circular tubes over a radiused die is influenced by several parameters including geometrical parameters of FGT tube same as angle α and exponent gradient of thickness distribution m, filet radius of die r, and coefficient of friction μ_d between die and tube. In the following, the effect of these parameters will be studied on the energy absorbing capacity of the FGT inversion tubes.

3.2.1 Effect of die radius r and coefficient of friction μ_d

The die geometry and lubricant effect on crush behavior of FGT tubes compared with the UT tubes. In all simulations thickness of UT tubes is selected 1.5mm.

Figure 11 depicts the effect of die radius on the response of FGT tubes. To strengthen the obtained results, Table 3 presentsP_{max}, P_m, E and SEA of the investigated tubes for various α angle and die radius r. Here, the coefficient of friction μ_d between die and tube are kept constant at 0.02. It is evident from Figure 11 that there is no significant change in the load–displacement response when the die radius is greater than 4 mm.

In the next step, the effect of coefficient of friction μ_d on the axial response of FGT tubes is found and compared with the UT tubes. The die radius and the UT tube thickness are chosen 2.5 mm and 2 mm, respectively. Figure 12 compares P_{max} and SEA of different FGT tubes with respect to coefficient of friction μ_d for final crush length of 40 mm. The peak force of each tube notably increases as the μ_d increase. However, it is seen that the energy absorption of FGT tube decreases for higher coefficient of friction μ_d , and is less influenced by the coefficient of friction μ_d and tends to decrease or remain constant for a given coefficient.

Power System Technology
ISSN:1000-3673

Received: 16-01-2024 Revised: 12-02-2024 Accepted: 27-03-2024

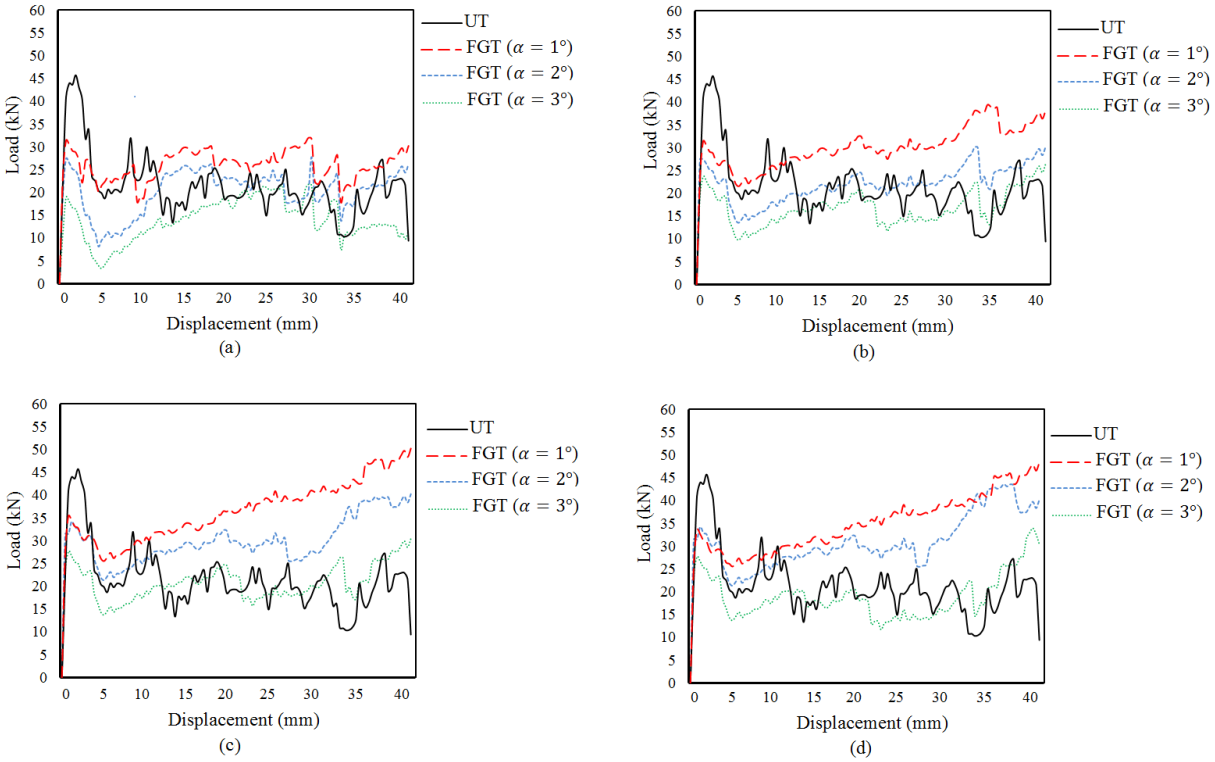

Figure 11. Load-displacement curves depicted the effect of die radius r on the response of FGT tubes, (a) $r = 1\ mm$, (b) $r = 2\ mm$, (c) $r = 4\ mm$, (d) $r = 6\ mm$

Table 3. FE simulation results of the investigated tubes for various lathe angles α and die radius r

Tube Case	$P_{max}(kN)$	$P_m(kN)$	E (kJ)	SEA(kJ/kg)
UT	47.3	28.8	1.15	33.5
FGT $(\alpha = 1°, r = 1mm)$	33.2	32.4	1.44	38.4
FGT $(\alpha = 2°, r = 1mm)$	27.4	24.5	0.98	32.4
FGT $(\alpha = 3°, r = 1mm)$	24.7	19.4	0.73	27.1
FGT $(\alpha = 1°, r = 2mm)$	38.8	34.1	1.36	36.9
FGT $(\alpha = 2°, r = 2mm)$	31.4	25.7	1.04	33.8
FGT $(\alpha = 3°, r = 2mm)$	27.6	23.7	0.84	29.6
FGT	51.2	39.5	2.18	44.7

Power System Technology
ISSN:1000-3673
Received: 16-01-2024 Revised: 12-02-2024 Accepted: 27-03-2024

$(\alpha = 1°, r = 4mm)$				
FGT $(\alpha = 2°, r = 4mm)$	39.2	32.8	1.35	37.2
FGT $(\alpha = 3°, r = 4mm)$	31.6	24.1	1.02	31.4
FGT $(\alpha = 1°, r = 6mm)$	48.9	37.4	2.01	41.8
FGT $(\alpha = 2°, r = 6mm)$	44.2	35.4	1.61	39.6
FGT $(\alpha = 3°, r = 6mm)$	38.6	22.4	0.96	30.8

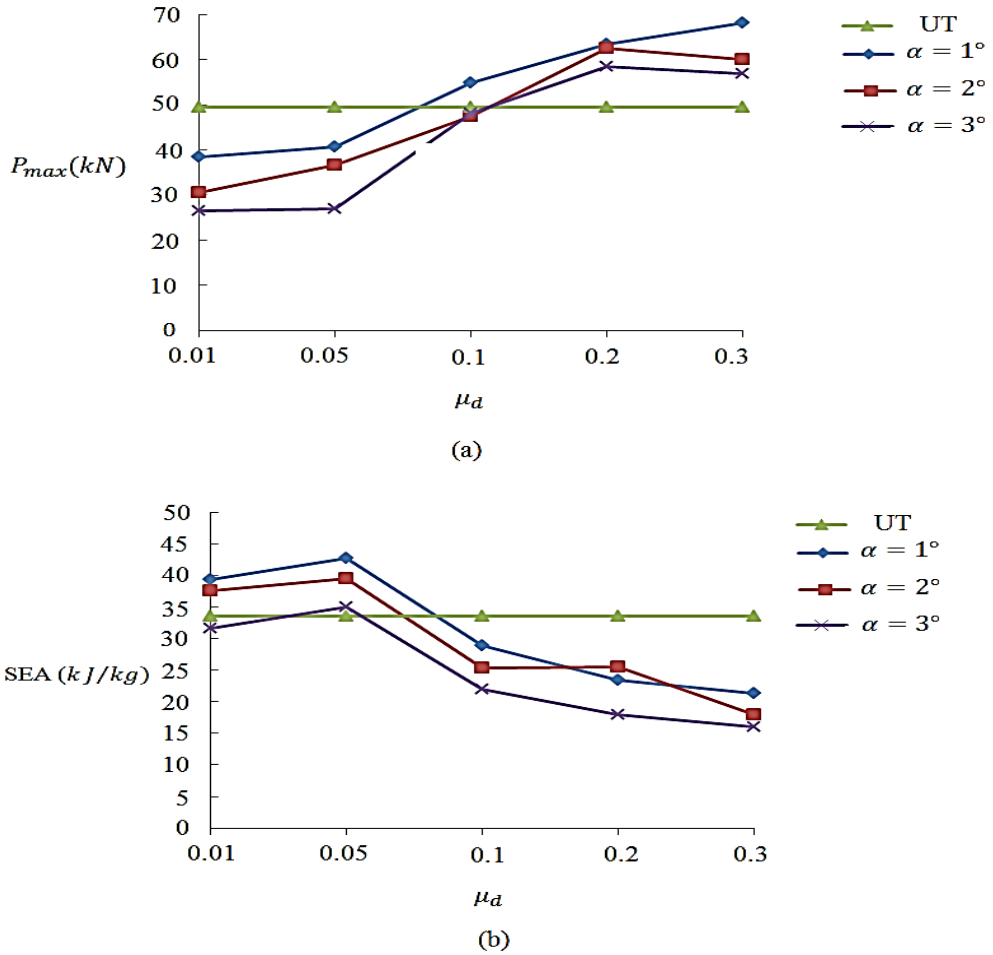

Figure 12. Comparison of (a) P_{max} vs. μ_d , (b) SEA vs. μ_d, curves for various lathe angles α

Power System Technology
ISSN:1000-3673
Received: 16-01-2024 Revised: 12-02-2024 Accepted: 27-03-2024

3.2.2 Effect of thickness distribution exponent gradient m

By varying the thickness distribution exponent gradient m, the crush response and energy absorption of inversion tubes are computed. Here, the tube and die main dimensions are considered as $t_1 = 1$ mm, $t_2 = 3$ mm and height L=75 mm, die fillet radius $r = 4$ mm, and coefficient of friction $\mu_d = 0.02$ and crushing velocity is selected as 3 mm/min.

According to Equation (1), in FGT tube, the thickness of the tube increases from t_1 the minimum value at the bottom to the maximum value at the top and the density function is concave for the value of exponent gradient $m > 1$ and is convex for the value of exponent gradient $m < 1$ (Figure 13). The influence of thickness distribution exponent gradient *m* across the range of SEA and peak force is evaluated in Table 4. It can be seen that SEA of the FGT tubes in inversion is greater than that of the corresponding UT tubes when m is greater than 1. However, an opposite result is observed when m is less than 1. Therefore, parameter m that controls the variation of thickness has significant influence on SEA. The term SEA monotonously increases in the region in which *m* are between 7 and 10. The maximum load of FGT decreases with the increasing of *m*. Therefore, variation of exponent *m* has significant role on the crashworthiness of the FGT tubes and *m>1* is a suitable choice for crashworthiness design.

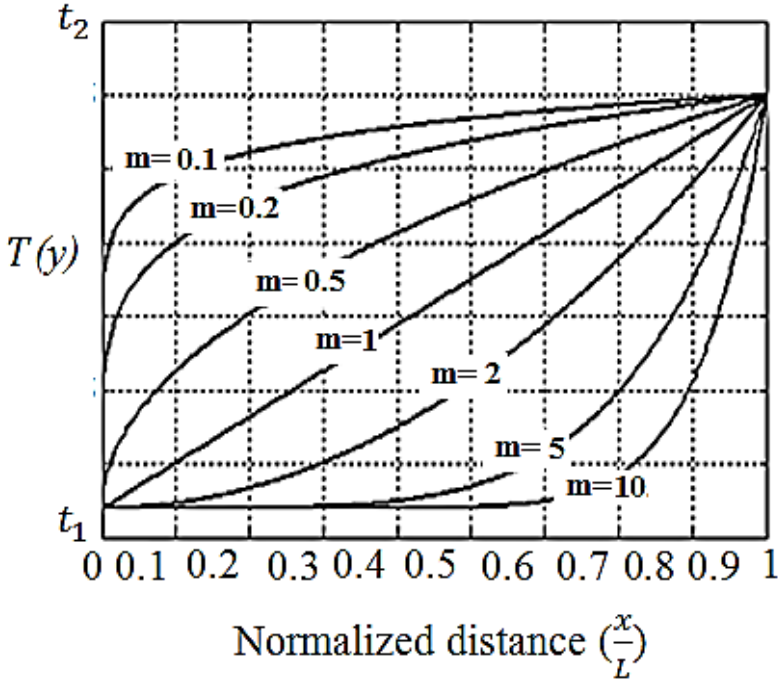

Figure 13.Variation in Thickness vs. normalized distance in nonlinear distribution of thickness

Power System Technology
ISSN:1000-3673
Received: 16-01-2024 Revised: 12-02-2024 Accepted: 27-03-2024

Table 4. The influence of thickness distribution exponent gradient m on crashworthiness parameters in FGT tubes

Tube Case	P_{max}(kN)	P_m(kN)	E (kJ)	SEA(kJ/kg)
UT	49.8	29.1	1.25	31.5
FGT ($m = 0.1$)	56.3	28.4	1.04	30.4
FGT ($m = 0.2$)	53.1	27.5	1.09	30.4
FGT ($m = 0.5$)	52.9	27.4	1.13	27.1
FGT ($m = 0.7$)	50.1	27.1	1.16	30.9
FGT ($m = 1$)	47.3	33.7	1.34	31.8
FGT ($m = 2$)	47.8	33.7	1.44	39.6
FGT ($m = 5$)	46.9	39.5	2.08	41.9
FGT ($m = 7$)	39.2	40.1	2.45	49.2
FGT ($m = 10$)	39.6	42.1	2.72	55.3

3.3 Dynamic Loading

Quasi-static test is not able to express actual crashworthy structure behavior. The explicit finite element procedure was used to analyze the dynamic response of UT and FGT inversion tubes subjected to axial impact loading. The numerical model was used to calculate energy absorption as a mass impacting the circular tube with different velocities. The calculated absorbed energy is compared with the corresponding results obtained for quasi-static simulation. In this study, Dynamic Amplification Factor (DAF) was used to consider the dynamic effect of crash. The term DAF relates quasi-static and dynamic responses to each other and is defined as the ratio of the absorbed energy under dynamic loading to the absorbed energy under quasi-static loading [2]. The effect of strain rate on the yield stress is described by Equation (3), whose parameters are mentioned in section 2.3 for D and q.

Power System Technology
ISSN:1000-3673
Received: 16-01-2024 Revised: 12-02-2024 Accepted: 27-03-2024

3.3.1 *Comparison of DAF in UT and FGT inversion tubes with linear thickness distribution ($m = 1$)*

Here, the effect of impact velocity on the DAF of absorbed energy for the UT (t=2mm) and FGT inversion tubes with $t_1 = 1$ mm, $t_2 = 3$ mm, die geometry $r = 4$ mm, and coefficient of friction $\mu_d = 0.02$. The numerical model was used to calculate energy absorption of a mass impacting the circular tube with different velocities. The calculated absorbed energy for FGT tubes with various angles α is compared with the corresponding results obtained for UT tubes. As it is seen in Figure 14, the term DAF have higher values for FGT tubes with angles $\alpha = 1°, 2°$. This is due to higher length of variable thickness part of the tubes, which results more complete inversion process. As an important conclusion, selecting suitable geometry for FGT tube and die can effectively control the amount of energy absorption under dynamic loading. Therefore, using FGT tubes is preferred for inversion process when dynamic loading must be increased for a desired value.

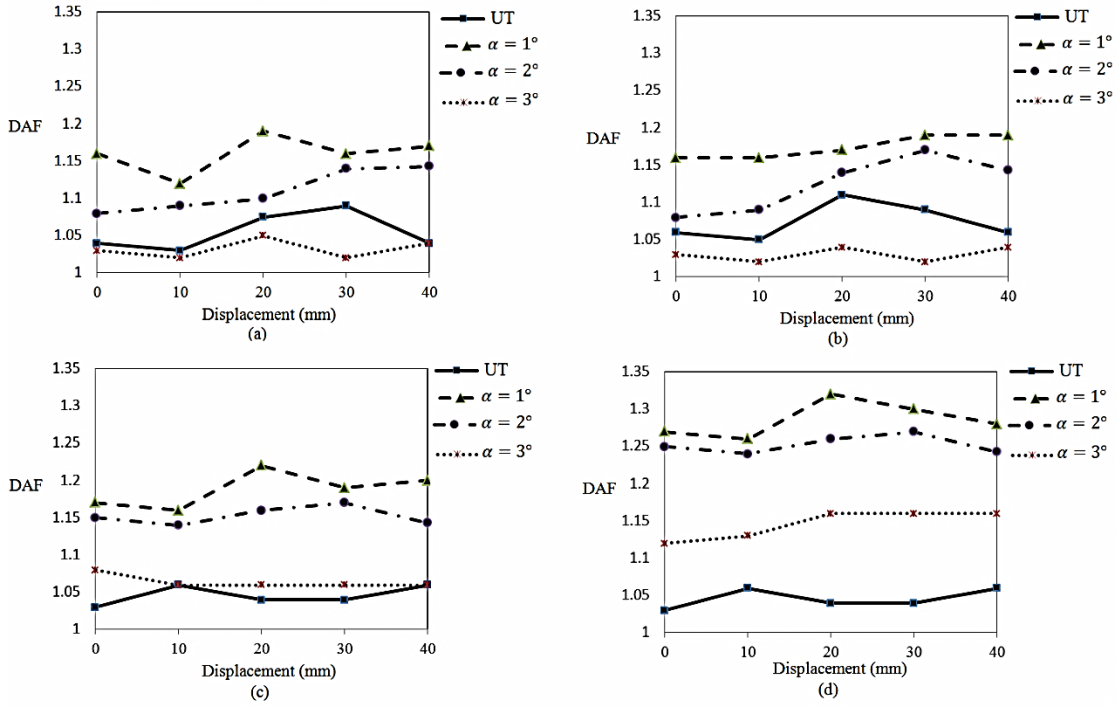

Figure 14.The effect of impact velocity on DAF for UT and FGT with various lathe angles α , (a)$v = 5\,m/s$, (b) $v = 10\,m/s$, (c) $v = 20\,m/s$, (c) $v = 30\,m/s$.

3.3.2 *Comparison of DAF in UT and FGT inversion tubes with nonlinear thickness distribution*

Here, the influence of nonlinear thickness distribution of FGT tubes under various loading velocities is established. The dynamic response and energy absorption of each tube was initially compared for different load speeds and thickness distribution exponent gradient *m*. The FGT

Power System Technology
ISSN:1000-3673
Received: 16-01-2024 Revised: 12-02-2024 Accepted: 27-03-2024

tubes have main dimensions are $t_1 = 1$ mm, $t_2 = 3$ mm, die geometry $r = 4$ mm, and coefficient of friction $\mu_d = 0.02$. Figure 15 shows significant effect of exponent gradient m on the DAF for both UT and FGT tubes. The results show that dynamic energy absorption property of concave distribution of thickness $m > 1$ is better than the convex pattern $m < 1$. This effect can be related to the smoothly rising in the load-displacement of the FGT tube, rising the interaction between the tube and die and the higher plastic energy damping of concave FGT structures.

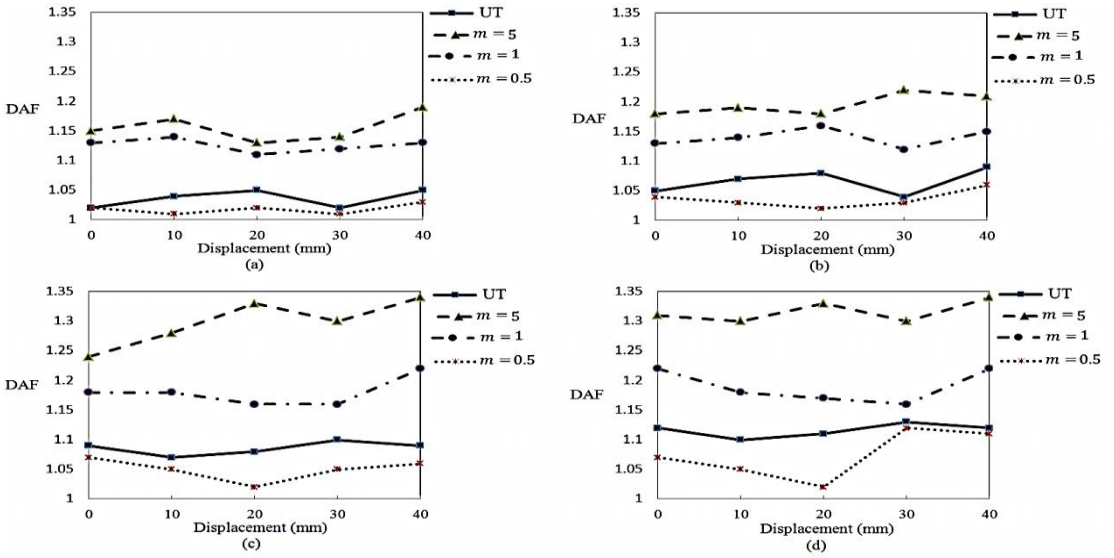

Figure 15.The effect of impact velocity on DAF for UT and FGT with various exponent gradient m, (a) $v = 5\,m/s$, (b) $v = 10\,m/s$, (c) $v = 20\,m/s$, (c) $v = 30\,m/s$.

4. Conclusion

The effect of thickness variation on the crushing response and energy absorption characteristics for inversion of thin-walled FGT tubes is investigated. In this study, both experimental tests and finite element simulations are employed. Experimental and FE analysis results indicate that selecting suitable geometry for the FGT tubes and the die produces full inversion crush response with higher energy absorption capacity with respect to their equivalent UT tubes. Energy absorption response was quantified with respect to different parameters same as die filet radius, coefficient of friction between tube and die, and thickness variation pattern of the FGT tube. The results have demonstrated the feasibility and superior performance of FGT tubes as energy absorbers. The primary conclusions and design information from the study are summarized as below:

(1) The experimental tests show that thickness variation pattern has significant influence on force responses and deformation model of FGT tubes. When interaction surface between FGT tube and inversion die is lubricated, the inversion process occurs more

Power System Technology
ISSN:1000-3673
Received: 16-01-2024 Revised: 12-02-2024 Accepted: 27-03-2024

completely. Thus, force response curves are smoother and can effectively dissipate more energy.

(2) Friction between the die and tube interfaces plays a key role in the overall development of inversion process. In fact, by changing this parameter a successful inversion mode of deformation easily changed into an undesired tube crush mode. A quantitative analysis shows that the reduction of friction coefficient less than 0.04 during inversion leads to the severe increasing of crashworthiness performance.

(3) Die radius can be effectively used as a parameter to control the amplification of dynamic response under dynamic loading. It can also be concluded that decreasing the die radius significantly decreases the SEA of the crush process.

References

[1] Hanssen AG, Langseth M, Hopperstad OS. Static and dynamic crushing of square aluminium extrusions with aluminium foam filler. Int J Impact Eng 2000;24(4):347–83.

[2] Ahmad Z, Thambiratnam DP. Application of foam-filled conical tubes in enhancing the crashworthiness performance of vehicle protective structures. Int J Crashworthiness 2009;14(4):349–63.

[3] Ahmad Z, Thambiratnam DP. Crushing response of foam-filled conical tubes under quasi-static axial loading. Mater Des 2009;30(7):2393–403.

[4] Aktay L, Kröplin BH, Toksoy AK, Güden M. Finite element and coupled finite element/smooth particle hydrodynamics modeling of the quasi-static crushing of empty and foam-filled single, bi tubular and constraint hexagonal- and square-packed aluminum tubes. Mater Des 2008 ;29(5):952–62.

[5] Mirfendereski L, Salimi M, Ziaei-Rad S. Parametric study and numerical analysis of empty and foam-filled thin-walled tubes under static and dynamic loadings. Int J Mech Sci 2008;50(6):1042–57.

[6] Zhang X., Cheng G., You Z., Zhang H., Energy absorption of axially compressed thin-walled square tubes with patterns, Thin Walled Struct. 45 (9) (2007) 737–746.

[7] Zhang X., Huh H., Energy absorption of longitudinally grooved square tubes under axial compression, Thin Walled Struct. 47 (12) (2009) 1469–1477.

[8] Saleh ghaffari S., Tajdari M., Panahi M., Mokhtarnezhad F., Attempts to improve energy absorption characteristics of circular metal tubes subjected to axial loading, Thin Walled Struct. 48 (6) (2010) 379–390.

[9] Zhang X., Zhang H., Energy absorption of multi-cell stub columns under axial compression, Thin Walled Struct. 68 (0) (2013) 156–163.

[10] Zhang X., Zhang H., Axial crushing of circular multi-cell columns, Int. J. Impact Eng. 65 (0) (2014) 110–125.

Power System Technology
ISSN:1000-3673
Received: 16-01-2024 Revised: 12-02-2024 Accepted: 27-03-2024

[11] Mohammadiha O., Ghariblu H., Crush behavior optimization of multi-tubes filled by functionally graded foam, Thin Walled Struct 2016;98:627–639.
[12] Sun GY, Li GY, Hou SJ, Zhou SW, Li W, Li Q. Crashworthiness design for functionally graded foam-filled thin-walled structures. Mater Sci Eng A 2010;527(7–8):1911–9.
[13] Zhang H., Zahng X., Crashworthiness performance of conical tubes with nonlinear thickness distribution, Thin Walled Struct 2016; 99:35–44.
[14] Al-Hassani STS, Johnson W, Lowe WT. Characterization of inversion tubes under axial loading. Journal of Mechanical Engineering Sciences 1972;14: 370–81.
[15] Reddy TY. Guist and Marble revisited—on the natural knuckle radius in tube inversion. International Journal of Mechanical Sciences 1992;34(10):761–8.
[16] Guist LR, Marble DP, Prediction of the inversion load of a circular tube. NASA TND 3622, 1966.
[17] Al-Hassani S.T.S., Johnson W., Lowe W., Characteristics of inversion tubes under axial loading, J. Mech. Eng. Sci. 14 (1972) 370–381.
[18] Karagiozova D, Alves M, Jones N. Inertia effects in axisymmetrically deformed cylindrical shells under axial impact. International Journal of Impact Engineering 2000;24:1083–115.
[19] T.Y. Reddy, Guist and Marble revisited—on the natural knuckle radius in tube inversion, Int. J. Mech. Sci. 34 (1992) 761–768.
[20] Miscow PC, AL-Qureshi HA. Mechanics of static and dynamic inversion processes. Int J Mech Sci 1997;39:147–61.
[21] Colokoglu A, Reddy TY. Strain rate and inertial effects in free external inversion of tubes. International Journal of Crashworthiness 1996;1(1): 93–106.
[22] Sekhon G.S., Gupta N.K., Guputa P.K., An analysis of external inversion of round tubes, J. Mater. Process. Technol. 2003;133:243–256.
[23] P.A. Rosa, R.M.O. Baptista, J.M.C. Rodrigues, P.A.F. Martins, Martins An investigation on the external inversion of thin-walled tubes using a die, Int. J. Plas. 2004;20:1931–1946.
[24] ASTM Standard E8/E8M-08. Standart test methods for tension testing of metallic materials. In: ASTM international, PA: West Conshohocken; 2003.
[25] Zarei H., Kroger M. 'Optimum honeycomb filled crash absorber design'. Mater. Des. 2008; 29(1):193–204.
[26] Liao X.T., Li Q, Yang X.J., Zhang W.G., Li W. Multiobjective optimization for crash safety design of vehicles using stepwise regression model'. Struct. Multidisc. Optim., 2008; 35: 561-569.
[27] Hou SJ, Li Q, Long SY, Yang XJ, Li W. Multiobjective optimization of multi-cell sections for the crashworthiness design. International Journal of Impact Engineering. 2008;35(11):1355–67